NIH-PA Author Manuscript

NIH-PA Author Manuscript

NIH-PA Author Manuscript

Brain Regions Associated with the Expression and Contextual Regulation of Anxiety in Primates

Ned H. Kalin, **Steven E. Shelton**, **Andrew S. Fox**, **Terrence R. Oakes**, and **Richard J. Davidson**
From the Department of Psychiatry (NHK, SES, ASF, RJD), Department of Psychology (NHK, RJD), and Waisman Laboratory for Brain Imaging and Behavior (NHK, ASF, TRO, RJD), University of Wisconsin-Madison, Madison, Wisconsin.

Abstract

Background— A key to successful adaptation is the ability to regulate emotional responses in relation to changing environmental demands or contexts.

Methods— High-resolution PET [18]fluoro-deoxyglucose (FDG) scanning in rhesus monkeys was performed during two contexts (alone, and human intruder with no eye contact) during which the duration of anxiety related freezing behavior was assessed. Correlations between individual differences in freezing duration and brain activity were performed for each of the two conditions, as well as for the contextual regulation between the two conditions.

Results— In both conditions, activity in the basal forebrain, including the bed nucleus of the stria terminalis and the nucleus accumbens were correlated with individual differences in freezing duration. In contrast, individual differences in the ability to regulate freezing behavior between contexts were correlated with activity in the dorsal anterior cingulate cortex, the thalamus and the dorsal raphe nucleus.

Conclusions— These findings demonstrate differences in the neural circuitry mediating the expression compared to the contextual regulation of freezing behavior. These findings are relevant since altered regulatory processes may underlie anxiety disorders.

Keywords

Anxiety; freezing; PET; monkey; emotion; regulation

The adaptive expression of emotion relates to the ability to regulate emotional responses as environmental or contextual demands change (Kalin and Shelton 1989; Davidson et al 2000; Kalin and Shelton 2003). Furthermore, it is likely that there are differences in the neural circuitry underlying the regulation, compared to the expression of emotion (Davidson et al 2000; Kalin and Shelton 2003; Morgan and LeDoux 1999; Ochsner et al 2002). Previously, we demonstrated that rhesus monkeys provide an excellent model to study mechanisms underlying human anxiety, its regulation, and anxiety-related psychopathology (Kalin 1993).

When threatened, primates commonly engage in behavioral inhibition or freezing behavior. Freezing is an automatic response characterized by the cessation of motor and vocal activity. In monkeys, individual differences in freezing duration are stable over time and reflect individual levels of anxiety (Kalin and Shelton 1989). Adaptive freezing helps an individual remain inconspicuous and decreases the likelihood of predatorial attack; however, excessive

---

freezing, or behavioral inhibition, is a risk factor for the development of anxiety disorders (Kagan et al 1998; Biederman et al 2001).

The human intruder paradigm was developed to study primates' defensive behaviors, such as freezing, and their regulation in response to changing environmental demands (Kalin and Shelton 1989). In this regard, it is informative to compare monkeys' responses elicited by attachment bond disruption occurring during the alone condition (ALN) with the responses elicited by threat occurring during the no eye contact condition (NEC). During ALN, monkeys are separated from their cagemates into a novel environment. Initially, monkeys display some freezing which functions to decrease the chances of detection by a potential predator. Once the monkey establishes that in the ALN environment there is no real predatorial threat, it locomotes and emits coo calls. These behaviors increase the likelihood of reunion by attracting the attention of conspecifics. Compared to ALN, the NEC condition provides a very different context introducing a direct threat. During NEC, the monkeys are exposed to a human intruder that presents her profile to the monkeys while avoiding eye contact. The lack of eye contact increases the uncertainty of the potential predator's intent and as a result the monkey engages in longer durations of freezing. This increased freezing compared to that during the ALN condition reflects the monkey's ability to adaptively regulate its anxiety-related behavior.

To understand the neural circuitry associated with freezing and its contextual regulation, [18]fluoro-deoxyglucose (FDG) PET scans were performed in monkeys exposed to the ALN and NEC conditions on separate days. FDG was selected as the radiotracer because its uptake into brain regions reflects brain metabolic activity (Sokoloff et al 1977; Phelps et al 1979). FDG was administered immediately before placing the monkeys in ALN or NEC conditions in which they remained for 30 min.

Based on previous work, we expected that individual differences in freezing duration would be correlated with activity in the amygdala, bed nucleus of the stria terminalis (BNST), and the periaqueductal gray (Davis et al 1997; LeDoux et al 1988; Davis 2000; Kalin et al 2004). To assess brain regions involved in the regulation of freezing, the change in freezing behavior between ALN and NEC was measured for each animal, and was correlated with changes in brain activity between these conditions. We hypothesized that individual differences in the regulation of freezing would be associated with the activation of regions of the prefrontal and anterior cingulate cortex (Ochsner et al 2002).

Methods and Materials

Subjects

Twenty-five male rhesus monkeys (M. mulatta) ranging in age from 2.2 to 4.6 years (mean age = 3.1 years) and weighing between 3.2 and 7.4 kg (mean weight = 5.0 kg) were the subjects. The monkeys were pair housed and maintained on a 12-hour light/dark cycle at the Wisconsin National Primate Research Center and at the Harlow Primate Laboratory. Animals had water ad libitum and were fed monkey chow every morning. Animal housing and experimental procedures were in accordance with institutional guidelines.

Magnetic Resonance Imaging Methods

Magnetic resonance imaging (MRI) data were available from 6 of the monkeys. Data were collected using a G E Signa 3T scanner (GE Medical Systems, Milwaukee, Wisconsin) with a standard quadrature birdcage headcoil. Whole brain anatomical images were acquired using an axial 3D T1-weighted inversion-recovery fast gradient echo sequence (TR = 9.4 msec, TE 2.1 msec, FOV = 14 cm, flip angle = 10°, NEX = 2, matrix = 512 × 512, voxel size = .3 mm, 248 slices, slice thickness = 1 mm, slice gap = −.05 mm, prep time = 600, bandwidth = 15.63,

frequency = 256, phase = 224). Before undergoing MRI acquisition, the monkeys were anesthetized with intramuscular ketamine (15 mg/kg).

PET Scan Protocol

To minimize the nonspecific effects of handling, the animals were handled, restrained and given a mock injection, and placed in the test cage for 30 min on 5 different days. After adaptation, each animal was scanned on 3 separate occasions after exposure to one of the conditions of the modified human intruder paradigm (Kalin and Shelton 1989). In this report, we present data from the ALN and NEC conditions. Data from the stare condition is not presented at this time because of our interest in understanding the regulation of freezing between the ALN and NEC conditions. Scans were not performed more frequently than once per week with 14 animals exposed to ALN first and 11 animals exposed to NEC first. The animals were food deprived overnight and between 8:00 am and 1:40 pm, the subjects were injected with <10 milliCuries (mCi) of the radiotracer FDG through a 1 9 ga intravenous (IV) catheter in the saphenous vein. Because greater than 70% of FDG uptake occurs within 30–40 min after injection (see e.g. Rilling et al 2001), the animals were immediately exposed to the paradigm and remained in the experimental conditions for 30 min. After each experimental session, the monkeys were anesthetized with ketamine followed by isofluorane gas, and their local glucose metabolism was assessed. Though previous studies demonstrate that ketamine (Langsjo et al 2003, 2004; Holcomb et al 2001; Freo and Ori 2004; Honey et al 2004) and isofluorane (Alkire et al 1997) produce changes in metabolism or rCBF in a variety of species (rats monkeys, humans), they all demonstrate that the response within a brain region is relatively constant across subjects. It is important to note that similar experimental timing was used for all subjects and that the anesthesia was identical in both conditions. During ALN, the monkeys remained alone in the test cage for the entire 30-min period. During NEC, the monkeys were place in the same cage for the entire 30-min period while a human entered the room for 10 min and presented her profile to the monkey, standing 2.5 meters from the cage and avoiding eye contact with the animal. To reduce the effects of habituation, the human left the test room for 5 min, reentered for 5 min, left again for 5 min, and reentered again for 5 min. Behaviors were recorded on videotape and were rated with a computerized scoring system by trained raters unaware of the treatment conditions (Kalin and Shelton 1989). Freezing was defined as a complete cessation of movement with the exception of vigilant eye movements that lasted for a minimum of three sec (Kalin and Shelton 1989). Following the Human Intruder conditions the animals were anesthetized with ketamine (15 mg/kg) and were administered intramuscular atropine sulfate (.27 mg). They were then fitted with an endotracheal tube, to administer 1–2% isofluorane gas anesthesia. The subject's head was positioned in a stereotaxic apparatus, to maintain the exact same head position between conditions. The animal was then placed in the P4 microPET scanner (Concorde Microsystems, Inc., Knoxville, Tennessee), a well characterized imaging system (Chatziioannou et al 1999, 2000; Cherry et al 1997; Farquhar et al 1998; Knoess et al 2003). The 60-min emission scan was started on average 67 min (range, 58–83 min) after injection of FDG. Heart rate, SpO_2, and respirations were monitored continuously. The delay between the activation paradigm and the time to scan, does not affect the relative metabolic activity among brain regions since with single bolus injections, FDG decays at the same rate in all parts of the brain. The microPET scanner has a reconstructed resolution of 2 mm full width at half maximum (FWHM) yielding a volumetric resolution of approximately 8 mm[3].

Post Acquisition Processing

To compare data across subjects, each PET scan was transformed into the same coordinate system using standard analysis methodology. A crucial aspect of whole brain inter-subject comparisons is to obtain an accurate fit of the brains from all subjects into the same coordinate space, such that each brain structure resides in the same location for all subjects. A multistage

process was used to create study-specific MRI and PET templates and accurately align each PET scan to the PET template. To facilitate the creation of an MRI template, each MRI scan was segmented into brain and nonbrain tissue, so that differences in skull and muscular anatomy would not influence the fit of the brain. One MRI image was manually transformed into a standard "template space" as defined by Paxinos et al (2000). The remaining MRIs were transformed linearly to match the one standardized image with a shift, a rotation, and a zoom transformation in each of the three (x, y, z) dimensions using AIR (9-parameter model) (Woods et al 1998). For each of the six subjects with MRI scans, reconstructed FDG images were transformed linearly via a shift and a rotation transformation in each of three-dimensions (x, y, z) to match their original MRIs (6-parameter rigid-body model). The 9-parameter transformations attained from the MRI transformations were then applied to the PET data, which were averaged to create a PET template in standardized space. This template was then masked to include the brain and surrounding muscles that bordered the brain, yielding a BRAIN-PET template. All subjects exhibited a similar pattern of extra-brain activity.

PET images from each subject were then matched to the template image. First, reconstructed PET images from each subject were smoothed with a 4 mm FWHM Gaussian kernel to accommodate small differences in the locations of functional regions across subjects (e.g. due to differences in gyral features) and increase the signal to noise ratio (Worsley et al 1996). Each PET image was then transformed into template space using a shift, a rotation, a zoom, and a perspective transformation in each of the three dimensions (x, y, and z) to match the location of the brain to the unmasked PET template using FSL (12-parameter affine model) (Jenkinson et al 2002). This transformation matched the size, location and orientation of each brain to that of the PET template. Each PET image was masked to exclude obvious nonbrain areas using the same mask applied to the BRAIN-PET template. Since posterior brain areas were not acquired for some scans due to the small field of view in the PET scanner and these areas were not of particular interest for this study, these areas were masked in both subject and template images. To more accurately align individual structures, images were warped to match the BRAIN-PET template using nonlinear transformations attained via a sixty-parameter model (Woods et al 1998). This method, with the addition of the MRI template, allowed for a clear distinction between brain and nonbrain activations. Each step of the registration was manually verified and final images were investigated in detail. Explicit validations for the NEC condition revealed that among thirteen control points within the brain (anterior point, posterior point, right posterior ventricle, and bilateral brain edges, putamen, caudate, and central white-matter landmarks) the mean deviance was .462 mm (SD: .610 mm) and maximum and minimum deviations for the majority of the regions (9/13) under 1mm in any given plane.

Blood samples for FDG quantification were not taken since this would have interfered with the assessment of the naturalistic behaviors during FDG uptake. To facilitate intersubject comparisons, each image was given the same mean-value by applying a global scale factor to each scan. Global scale factors were determined by adjusting the mean, based on a partial brain ROI that excluded regions not collected for all subjects, to be constant across subjects (Carmargo et al 1992).

Data Analysis

There were four monkeys whose prefrontal areas were not within the PET scanner FOV for one of their two scans. As prefrontal areas were of particular interest, analyses for each condition were performed excluding subjects that lacked pre-frontal data (ALN: $n = 22$, NEC: $n = 24$, NEC-ALN: $n = 21$). Additionally, posterior brain areas were not acquired in some animals. Therefore, for all subjects, data from areas more than 20 mm posterior to the center of the anterior commissure (AC), portions of visual and parietal cortices, were excluded from analyses.

After accurate registration, each brain voxel represents the amount of metabolic activity in the same region across subjects. Statistical tests investigating the relationship between brain activity and freezing behavior were conducted separately for the NEC and ALN conditions as well as for the change between NEC and ALN conditions. The freezing data were not normally distributed, and were therefore log transformed. Since freezing and brain metabolism may be affected by age, age was controlled for in the brain activity-behavior analyses. To explore the relationship between freezing behavior and brain activity, each voxel in the brain was correlated with the log duration of freezing behavior within the NEC and ALN conditions, while controlling for age. Sets of connected voxels that significantly ($p < .005$, two-tailed uncorrected) correlated with freezing behavior were defined as clusters. Clusters within areas of interest were further examined by plotting their distribution to ensure results were not driven by outliers. This was done by first calculating the average value within the clusters of interest for each scan. The average values and log durations of freezing were then adjusted to account for age by performing a linear regression, with age the sole predictor, and calculating the residual values. To insure that the plots had meaningful ordinate and abscissa values, the residuals were converted to a standard normal distribution. To assign a single estimate of the amount of variance explained by the plotted data, a second linear regression was performed. This regression duplicated the voxelwise correlation, but produced a single statistical estimate of the variance that can be attributed to the brain activity-behavior relationship (reported R^2 values). This regression represents the zero-order correlation between standardized residual log duration of freezing behavior and standardized residual average values for clusters of interest. The same procedure was used to identify, process, and analyze the relationship between the change in brain activity and the change in freezing behavior across the NEC and ALN conditions. In this case, the results represent the zero-order correlation between the difference in log-transformed freezing duration between the NEC and ALN conditions and the differences in average brain activity between the NEC and ALN conditions in clusters of interest, after partialling age from each variable. For all analyses R^2 values represent the amount of variance that can be attributed to the brain activity-behavior relationship.

Results

Brain Activity and Freezing Duration During NEC and ALN Conditions

As can be seen in Figure 1, freezing occurred in both the ALN and NEC conditions with significantly more freezing expressed during NEC ($t = 2.594$, $p = .016$). During NEC, freezing duration was correlated with activation in an area of the basal forebrain that predominantly encompassed the bed nucleus of the stria terminalis (BNST), a portion of the substantia innominata and more anteriorly the shell of the nucleus accumbens (NAC) (this region will be referred to as BNST/NAC) ($R^2 = .511$, $p < .001$) (Figure 2). Figure 2 shows that this BNST/ NAC region was located in the right hemisphere (maximum t-value located at: x = 3.125 mm, y = 1.875 mm, z = −1.25 mm relative to the center of the anterior commissure). While no significant ($p < .005$, two-tailed uncorrected) correlations were found between amygdala activity and freezing behavior, decreasing the threshold to $p < .05$ (two-tailed uncorrected) revealed small regions in the right amygdala that were positively correlated with freezing occurring during both ALN and NEC. No significant correlation was found between activity in the periaqueductal gray brain stem region and freezing. Activation in motor cortex was negatively correlated with freezing duration ($R^2 = .506$, $p < .001$) (Figure 3). In addition, the BNST/NAC region that was correlated with freezing was negatively correlated with the motor cortex region that was correlated with freezing ($R^2 = .372$, $p < .001$). Other regions that were significantly correlated with freezing duration are displayed in Table 1.

To understand the extent to which the individual differences in BNST/NAC activity were specifically correlated with freezing and not other behaviors, activity from the BNST/NAC

region that was correlated with freezing during NEC was extracted and correlated with individual differences in the frequency of cooing occurring during NEC. In contrast to freezing, individual differences in cooing were not significantly correlated with BNST/NAC activity ($R^2 = .088$, $p = .158$). Furthermore, the correlation between BNST/NAC activity and freezing significantly differed from the correlation between BNST/NAC and cooing ($p < .017$).

Freezing behavior also occurred during the ALN condition, although with a significantly shorter duration. A voxelwise regression between freezing duration occurring during ALN and brain activity revealed that individual differences in freezing were positively correlated with a left basal forebrain region that encompassed the BNST, substantia innominata, shell of the nucleus accumbens, and some of the core of the nucleus accumbens ($R^2 = .477$, $p < .001$) (the maximum t-value located at: x = −4.375mm, y = 2.5mm, z = −.635mm relative to the center of the anterior commissure). Figure 2 demonstrates that the BNST/NAC regions that were correlated with freezing during the ALN and NEC conditions were in close proximity but appeared to be unilateral and on opposite sides of the brain. Since we expected that this effect would be bilateral and selecting threshold cut-points is arbitrary, we reanalyzed the data with a reduced statistical threshold. Moreover, presenting data with multiple statistical thresholds has been suggested as a method to more completely characterize brain-behavior relations (Jernigan et al 2003). Reduced thresholds ($p < .05$, 2-tailed) revealed that for both NEC and ALN conditions the BNST/NAC correlations were bilateral. Using the same threshold we found a bilateral BNST/NAC region (63.7 mm^3), common to the NEC and ALN conditions that was correlated with freezing in each condition. Brain activity in this region during NEC was positively correlated with NEC freezing duration ($R^2 = .570$, $p < .001$) and a similar correlation was found between ALN brain activity extracted from this region and ALN freezing duration ($R^2 = .450$, $p < .001$). To further examine this issue, we performed t-tests to determine if the lateralized BNST/NAC clusters from the NEC and ALN conditions and the bilateral combined BNST/NAC cluster differentially predicted freezing in either of the two conditions. No significant differences in the freezing and brain activity correlations were found when comparing the correlations with the more stringent BNST clusters (defined by the $p < .005$, two-tailed uncorrected threshold) with those from the combined BNST cluster (defined by $p < .05$, two-tailed uncorrected thresholds).

Similar to the NEC condition, motor cortex activity during ALN was negatively correlated with ALN freezing ($R^2 = .566$, $p < .001$) (Figure 3). Again, the BNST/NAC and motor cortex regions that were correlated with freezing during ALN were negatively correlated with each other ($R^2 = .185$, $p < .04$). Other significant regions that were correlated with freezing during ALN are displayed in Table 1.

Assessing Contextual Regulation: Changes in Brain Activity Between NEC and ALN in Relation to Changes in Freezing Between NEC and ALN

To identify brain regions that are associated with the ability to regulate freezing responses in relation to increasing threat, we subtracted brain activity and behavior during ALN from that occurring during NEC. This comparison is relevant because of the adaptive increase in freezing duration that occurs during NEC compared to ALN. Results demonstrated a significant positive correlation with: area 24c which is part of the dorsal anterior cingulate cortex ($R^2 = .627$, $p < .001$), an area of the brain stem encompassing the dorsal raphe ($R^2 = .484$, $p < .001$), and the lateral thalamus ($R^2 = .614$, $p < .001$) (Figure 4). Furthermore, when using the ROIs from the above regions, significant positive correlations were found between NEC-ALN brain activity in the brain stem region with the area 24c ($R^2 = .325$, $p < .01$) and thalamic regions ($R^2 = .504$, $p < .001$). The NEC-ALN activity in the thalamic region was also positively correlated with dorsal anterior cingulate cortex activity ($R^2 = .360$, $p < .001$)

There was a notable lack of correlation between the NEC-ALN changes in freezing duration with the NEC-ALN changes in BNST/NAC activity. In addition, no significant correlation was found between activity in the BNST/NAC region shared between the two conditions with NEC-ALN freezing. Other regions that were significantly correlated with the change in freezing are displayed in Table 2.

Discussion

The high-resolution, small-animal, PET scanner allowed us to examine patterns of brain activity in rhesus monkeys that are associated with freezing, as well as brain regions associated with the ability to adaptively regulate this threat-related response. The rhesus monkey is an excellent model because similar to humans, rhesus monkeys have a well-developed prefrontal cortex with bidirectional connections to the amygdala and other key subcortical structures (Amaral et al 1992; Fuster 1997). This is important because the functional linkage between regions of prefrontal cortex with the amygdala, and other limbic and brain stem regions, is hypothesized to underlie the processing and regulation of emotion (Davidson et al 2000; Davidson 2002; Kalin and Shelton 2003; Ochsner et al 2002).

The current findings highlight circuitry in the BNST/NAC that is strongly correlated with freezing duration in both the NEC and ALN conditions. Animals with greater metabolic activity in these regions display more freezing. These findings are consistent with rodent data implicating the BNST in anxiety (see Davis et al 1997). However, this circuitry is unrelated to the animal's capacity to regulate its freezing behavior as a function of context. While a small amount of freezing occurs at the beginning of the ALN condition, the overriding adaptive response when separated and alone is to engage in behaviors that result in reunion. In contrast, freezing is the critical adaptive response in the NEC condition serving to help the animal remain undiscovered in the face of potential predatorial threat. Animals with the greatest capacity to adaptively regulate their anxiety-related responses are those with the largest increase in freezing behavior between the ALN and the NEC conditions.

Examining the neural circuitry associated with changes in emotional behavior between contexts provides novel information about mechanisms underlying emotion regulation. While BNST/NAC activity correlated with freezing during both NEC and ALN, the change in freezing within subjects across the contexts was not correlated with activity in this region. This suggests involvement of other brain regions in the contextual regulation of freezing. The data demonstrate that animals with the largest change in freezing between contexts also have the greatest increases in metabolic activity in lateral thalamus, brain stem/dorsal raphe regions and area 24c, part of the dorsal anterior cingulate cortex. This underscores the differences in the neural circuitry that underlie the expression compared to the adaptive regulation of freezing.

Involvement of the thalamus in emotion regulation is consistent with its well-known function of integrating sensory information. The involvement of the dorsal raphe is interesting since it is the brainstem site from which the regulatory neurotransmitter serotonin emanates. The anterior cingulate cortex has been associated with error monitoring and is activated when individuals are confronted with competing tendencies (Carter et al 1998). Evidence suggests anatomical specialization within the anterior cingulate cortex such that the rostral anterior cingulate is associated with the affective domain (Salomons et al 2004), whereas the dorsal anterior cingulate is associated with cognitive and motor processes (Holroyd et al 2004; Devinsky et al 1995). Previous human neuroimaging research has underscored the importance of the rostral anterior cingulate cortex in emotion regulation (e.g., Davidson et al 2002; Ochsner et al 2002), however in the present study, activation of the rostral anterior cingulate was not associated with changes in freezing behavior. Anatomical studies in primates demonstrate that the region of the dorsal anterior cingulate cortex (area 24c) that we found to be associated with

the regulation of freezing has direct projections to motor cortex and to spinal cord regions involved with motor activity (Dum and Strick 2002). In addition, human fMRI studies suggest that area 24c is involved in integrating cognition with focused attention and motor behavior (Bush et al 1998; Paus 2001). Therefore, activation of this region may be involved in regulating fear or anxiety motivated changes in motor activity, or freezing, associated with changes in environment. The present experiment suggests that the dorsal anterior cingulate, along with other brain regions that it recruits, plays a role in adaptively adjusting anxiety-related behaviors. We previously demonstrated that monkeys that engage in high levels of freezing also have a characteristic pattern of physiological activation. These findings led us to propose the anxious endophenotype as a constellation of trait-like behavioral and physiological parameters that are associated with increased risk to develop anxiety disorders (Kalin and Shelton 2003). Using excitotoxic lesions in monkeys, we also found that the central nucleus of the amygdala is involved in modulating many of the parameters of the anxious endophenotype, including the expression of freezing (Kalin et al 2004). These findings led us to hypothesize that amygdala activation would be associated with freezing duration. While the relation between amygdala activity and freezing did not reach the statistical threshold, a weak positive association was found. Possible explanations for the lack of a more robust amygdala finding include the kinetics of FDG-PET and the well-characterized time-limited activation of the amygdala (e.g., Breiter et al 1996). In the present study, measures of regional glucose metabolism with PET were acquired over a 30-min period and therefore it would not be possible to detect transient changes in amygdala activation. Furthermore, in human studies that have used PET, rather than fMRI paradigms designed to assess activation patterns associated with anxiety, a similar lack of amygdala activation has been reported (e.g., Rauch et al 1997).

The results demonstrate a consistent association between individual differences in freezing duration and activation of the BNST/NAC region in the basal forebrain in both human intruder paradigm conditions, albeit the exact BNST/NAC regions for each condition were not identical. However, by creating an ROI that combined the BNST/NAC regions defined in the ALN and NEC, we demonstrated correlations between freezing duration occurring in each of the two conditions with brain activity in an identical BNST/NAC region. Moreover, this region that was strongly associated with freezing was not associated with other behaviors such as cooing indicating that this circuitry is specific to freezing. We also found a negative correlation between motor cortex activity and duration of freezing behavior in the two conditions. This was expected since freezing constitutes an inhibition of ongoing motor behavior.

Based on the concept of the central extended amygdala, it is of interest that we found an association between freezing and activation of the BNST/NAC basal forebrain structures. Anatomical, biochemical, and functional studies suggest that the central extended amygdala is comprised of the central nucleus of the amygdala and the BNST (Cassell et al 1999). The amygdala, including the central nucleus, directly projects to the BNST (Dong et al 2001; Amaral et al 1992). In addition, the anterior portions of the BNST project to and are continuous with the shell of the nucleus accumbens (Swanson and Cowan 1979; Heimer et al 1997). It has been suggested that this amygdala-BNST-accumbens shell network, which is highly connected to orbitofrontal cortex, thalamus, and brain stem, functions to integrate emotion, motivation, and behavior (Heimer et al 1997).

From work in rodents, it has been proposed that the BNST is important in mediating anxiety (Walker et al 2003). For example, temporary inactivation of the BNST in rats decreased freezing that was elicited by exposure to an odor of a natural predator (Fendt et al 2003). A dissociation between the functions of the central nucleus of the amygdala with those of the BNST has been suggested such that the central amygdala nucleus is thought to mediate brief responses to fearful stimuli, whereas the BNST has been hypothesized to mediate anxiety responses of considerably longer duration (Walker et al 2003). The BNST is also a site that

mediates the anxiogenic effects of the neuropeptide corticotrophin releasing factor (Lee and Davis 1997). Our data provide the first evidence suggesting that the BNST may play a role in modulating anxiety-related responses in primates.

The PET data also demonstrate that activation of the nucleus accumbens, predominately the shell, is associated with increased freezing. This is consistent with the close anatomical linkages between the BNST and the accumbens. In addition, many studies implicate the nucleus accumbens as part of the circuitry involved in mediating the effects of aversive stimuli and not simply selectively involved in mediating reward-associated behaviors (Schoenbaum and Setlow 2003; Yanagimoto and Maeda 2003). Using transgenic mice it has been shown that exposure to both appetitive and stressful stimuli increases cAMP response element mediated gene transcription in the accumbens shell (Barrot et al 2002). Furthermore, reductions in levels of the cAMP response element binding protein in the accumbens shell decreases behavioral responses to these stimuli (Barrot et al 2002). Finally, human functional imaging studies demonstrate activation of the nucleus accumbens in response to aversive stimuli (Zald and Pardo 2002; Paradisio et al 1999) and in assessing the salience and emotional relevance of stimuli (Phan et al 2004).

The adaptive expression of emotion and emotion-related behavior is related to the ability to regulate responses in relation to different environmental demands (Davidson et al 2000; Kalin and Shelton 2003). We previously demonstrated the utility of the human intruder paradigm in studying the regulation of fear and anxiety-related responses, and using this paradigm identified individual differences in monkeys' abilities to regulate freezing behavior (Kalin and Shelton 1989). Moreover, we and others proposed that an inability to adaptively regulate affective and anxiety responses may be a fundamental component of affective and anxiety disorders (Davidson et al 2000; Kalin and Shelton 2003). The findings from the current study highlight the different circuitry involved in the expression of freezing versus the adaptive regulation of freezing. Further studies in primates examining the circuitry involved in maladaptive patterns of anxiety regulation have the potential to yield insights related to the pathophysiology of anxiety and affective disorders. Drevets, 1999, Rauch et al., 2003, Walker and Davis, 1997
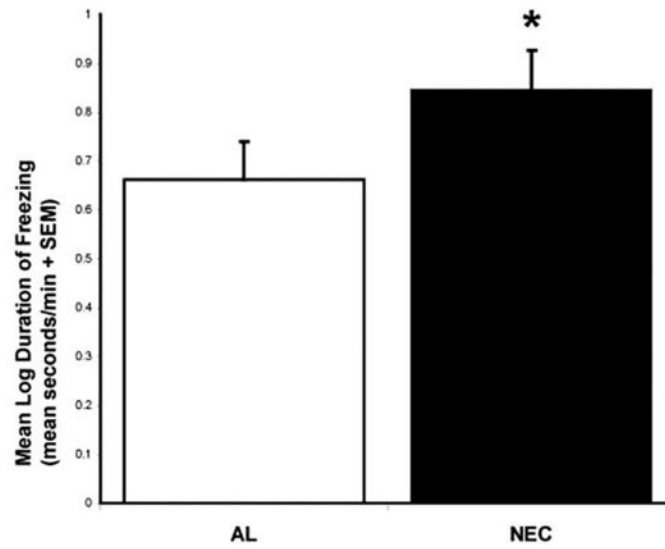
Acknowledgements

References

Alkire MT, Haier RJ, Shah NK, Anderson CT. Positron emission tomography study of regional cerebral metabolism in humans during isoflurane anesthesia. Anesthesiology 1997;86(3):549–557. [PubMed: 9066320]

Amaral, DG.; Price, JL.; Pitkanen, A.; Carmichael, ST. Anatomical organization of the primate amygdaloid complex. In: Aggleton, J., editor. The Amygdala. New York: Wiley-Liss; 1992. p. 1-67.

Barrot M, Olivier JD, Perrotti LI, DiLeone RJ, Berton O, Eisch AJ, et al. CREB activity in the nucleus accumbens shell controls gating of behavioral responses to emotional stimuli. Proc Natl Acad Sci USA 2002;99(17):11435–11440. [PubMed: 12165570]

Biederman J, Hirshfeld-Becker DR, Rosenbaum JF, Herot C, Friedman D, Snidman N, et al. Further evidence of association between behavioral inhibition and social anxiety in children. Am J Psychiatry 2001;158:1673–1679. [PubMed: 11579001]

Breiter HC, Etcoff NL, Whalen PJ, Kennedy WA, Rauch SL, Buckner RL, et al. Response and habituation of the human amygdala during visual processing of facial expression. Neuron 1996;17:875–887. [PubMed: 8938120]
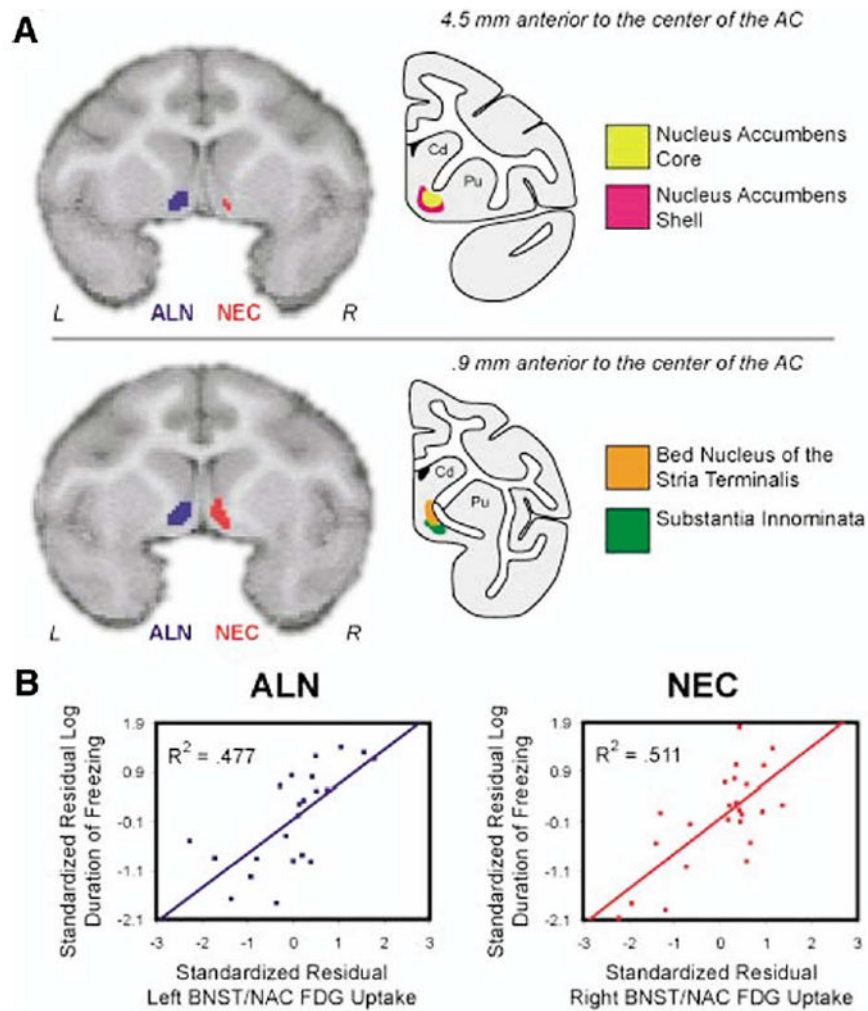
Bush G, Whalen PJ, Rosen BR, Jenike MA, McInerney SC, Rauch SL. The counting Stroop: an interference task specialized for functonal neuroimaging–validation study with functional MRI. Human Brain Mapping 1998;6:270–282. [PubMed: 9704265]

Camargo EE, Szabo Z, Links JM, Sostre S, Dannals RF, Wagner HN Jr. The influence of biological and technical factors on the variability of global and regional brain metabolism of 2-[18F]fluoro-2-deoxy-D-glucose. J Cereb Blood Flow Metab 1992;12(2):281–290. [PubMed: 1548300]

Carter CS, Braver TS, Barch DM, Botvinick MM, Noll D, Cohen JD. Anterior cingulate cortex, error detection, and the online monitoring of performance. Science 1998;280(5364):747–749. [PubMed: 9563953]

Cassell MD, Freedman LJ, Shi C. The intrinsic organization of the central extended amygdala. Ann N Y Acad Sci 1999;877:217–241. [PubMed: 10415652]

Chatziioannou A, Silverman RW, Meadors K, Farquhar TH, Cherry SR. Techniques to improve the spatial sampling of microPET - A high resolution animal PET tomograph. IEEE Trans Nucl Sci 2000;47:422–427.

Chatziioannou AF, Cherry SR, Shao Y, Silverman RW, Meadors K, Farquhar TH, et al. Performance evaluation of microPET: a highresolution lutetium oxyorthosilicate PET scanner for animal imaging. J Nucl Med 1999;40:1164–1175. [PubMed: 10405138]

Cherry SR, Shao Y, Silverman RW, Chatziioannou AF, Meadors K, Siegel S. MicroPET: a high resolution PET scanner for imaging small animals. IEEE Trans Nucl Sci 1997;44:1161–1166.

Davidson RJ. Anxiety and Affective Style: role of prefrontal cortex and amygdala. Biol Psychiatry 2002;51:68–80. [PubMed: 11801232]

Davidson RJ, Jackson DC, Kalin NH. Emotion, plasticity, context, and regulation: perspectives from affective neuroscience. Psych Bull 2000;126:890–909.

Davidson RJ, Lewis D, Alloy L, Amaral D, Bush G, Cohen JD, et al. Neural and behavioral substrates of mood and mood regulation. Biol Psychiatry 2002;52:478–502. [PubMed: 12361665]

Davis, M. The role of the amygdala in conditioned and unconditioned fear and anxiety. In: Aggleton, J., editor. The Amygdala. 2. New York: Oxford Press; 2000. p. 213-287.

Davis M, Walker DL, Lee Y. Amygdala and bed nucleus of the stria terminalis: differential roles in fear and anxiety measured with the acoustic startle reflex. Philos Tans R Soc London B Biol Sci 1997;352:1675–1687.

Devinsky O, Morrell MJ, Vogt BA. Contributions of anterior cingulate cortex to behaviour. Brain 1995;118(Pt 1):279–306. [PubMed: 7895011]

Dong H-W, Petrovich GD, Swanson LW. Topography of projections from amygdala to bed nuclei of the stria terminalis. Brain Research Reviews 2001;38:192. [PubMed: 11750933]

Drevets WC. Prefrontal cortical-amygdalar metabolism in major depression. Ann N Y Acad Sci 1999;877:614–637. [PubMed: 10415674]

Dum RP, Strick PL. Motor areas in the frontal lobe of the primate. Physiol Behav 2002;77(4–5):677–682. [PubMed: 12527018]

Farquhar TH, Chatziioannou A, Cherry SR. An evaluation of exact and approximate 3-D reconstruction algorithms for a high-resolution, small-animal PET scanner. IEEE Trans Med Imaging 1998;17:1073–1080. [PubMed: 10048864]

Fendt M, Endres T, Apfelbach R. Temporary inactivation of the bed nucleus of the stria terminalis but not of the amygdala blocks freezing induced by trimethylthiazoline, a component of fox feces. J Neurosci 2003;23(1):23–28. [PubMed: 12514197]

Freo U, Ori C. Effects of anesthesia and recovery from ketamine racemate and enantiomers on regional cerebral glucose metabolism in rats. Anesthesiology 2004;100(5):1172–1178. [PubMed: 15114215]

Fuster, JM. The Prefrontal Cortex: Anatomy, Physiology, and Neuropsychology of the Frontal Lobe. Philadelaphia: Lippincott-Raven; 1997.

Heimer L, Harlan RE, Alheid GF, Garcia MM, de Olmos J. Substantia innominata: a notion which impedes clinical-anatomical correlations in neuropsychiatric disorders. Neuroscience 1997;76(4):957–1006. [PubMed: 9027863]

Holcomb HH, Lahti AC, Medoff DR, Weiler M, Tamminga CA. Sequential regional cerebral blood flow brain scans using PET with (H2O)-O-15 demonstrate ketamine actions in CNS dynamically. Neuropsychopharmcology 2001;25(2):165–172.

Holroyd CB, Nieuwenhuis S, Yeung N, Nystrom L, Mars RB, Coles MG, et al. Dorsal anterior cingulate cortex shows fMRI response to internal and external signals. Nat Neurosci 2004;7:497–498. [PubMed: 15097995]

Honey RAE, Honey GD, O'Loughlin C, Sharar SR, Kumaran D, Bullmore ET, et al. Acute ketamine administration alters the brain responses to executive demands in a verbal working memory task: an fMRI study. Neuropsychopharmacology 2004;29(6):1203–1214. [PubMed: 15100698]

Jenkinson M, Bannister P, Brady J, Smith S. Improved optimisation for the robust and accurate linear registration and motion correction of brain images. Neuroimage 2002;17(2):825–841. [PubMed: 12377157]

Jernigan TL, Gamst AC, Fennema-Notestine C, Ostergaard AL. More "mapping" in brain mapping: statistical comparison of effects. Hum Brain Mapp 2003;19(2):90–95. [PubMed: 12768533]

Kagan J, Reznick JS, Snidman N. Biological bases of childhood shyness. Science 1988;240:167–171. [PubMed: 3353713]

Kalin NH. The neurobiology of fear. Sci Am 1993;268:94–101. [PubMed: 8386852]

Kalin NH, Shelton SE. Defensive behaviors in infant rhesus monkeys: environmental cues and neurochemical regulation. Science 1989;243:1718–1721. [PubMed: 2564702]

Kalin NH, Shelton SE. Nonhuman Primate models to study anxiety, emotion regulation and psychopathology. Ann NY Acad Sci 2003;1008:189–200. [PubMed: 14998885]

Kalin NH, Shelton SE, Davidson RJ. The role of the central nucleus of the amygdala in mediating fear and anxiety in the primate. J Neurosci 2004;24:5506–5515. [PubMed: 15201323]

Kalin NH, Shelton SE, Davidson RJ, Kelley AE. The primate amygdala mediates acute fear but not the behavioral and physiological components of anxious temperament. J Neurosci 2001;21:2067–2074. [PubMed: 11245690]

Knoess C, Siegel S, Smith A, Newport D, Richerzhagen N, Winkeler A, et al. Performance evaluation of the microPET R4 PET scanner for rodents. European J Nucl Med & Molecular Imaging 2003;30:737–747.

Langsjo JW, Kaisti KK, Aalto S, Hinkka S, Aantaa R, Oikonen V, et al. Effects of subanesthetic doses of ketamine on regional cerebral blood flow, oxygen consumption, and blood volume in humans. Anesthesiology 2003;99(3):614–623. [PubMed: 12960545]

Langsjo JW, Salmi E, Kaisti KK, Aalto S, Hinkka S, Aantaa R, et al. Effects of subanesthetic ketamine on regional cerebral glucose metabolism in humans. Anesthesiology 2004;100(5):1065–1071. [PubMed: 15114201]

LeDoux JE, Iwata J, Cicchetti P, Reis DJ. Different projections of the central amygdaloid nucleus mediate autonomic and behavioral correlates of conditioned fear. J Neurosci 1988;8:2517–2529. [PubMed: 2854842]

Lee Y, Davis M. Role of the hippocampus, the bed nucleus of the stria terminalis and the amygdala in the excitatory effect of corticotrophin-releasing hormone on the acoustic startle reflex. J Neurosci 1997;17:6434–6446. [PubMed: 9236251]

Morgan MA, LeDoux JE. Differential contribution of dorsal and ventral medial prefrontal cortex to the acquisition and extinction of conditioned fear in rats. Neurobiol Learn Mem 1999;72(3):244–251. [PubMed: 10536101]

Ochsner KN, Bunge SA, Gross JJ, Gabrieli JD. Rethinking feelings: an FMRI study of the cognitive regulation of emotion. J Cogn Neurosci 2002;14:1215–1229. [PubMed: 12495527]

Paradiso S, Johnson DL, Andreasen NC, O'Leary DS, Watkins GL, Ponto LL, et al. Cerebral blood flow changes associated with attribution of emotional valence to pleasant, unpleasant, and neutral visual stimuli in a PET study of normal subjects. Am J Psychiatry 1999;156:1618–1623. [PubMed: 10518175]

Paus T. Primate anterior cingulate cortex: where motor control, drive and cognition interface. Nat Rev Neurosci 2001;2(6):417–424. [PubMed: 11389475]

Paxinos, G.; Huang, X-F.; Toga, AW. The Rhesus Monkey Brain in Stereotaxic Coordinates. San Diego: Academic Press; 2000.

Phan KL, Taylor SF, Welsh RC, Ho S-H, Britton JC, Liberzon I. Neural correlates of individual ratings of emotional salience: a trial-related fMRI study. NeuroImage 2004;21:768–780. [PubMed: 14980580]

Phelps ME, Huang SC, Hoffman EJ, Selin C, Sokoloff L, Kuhl DE. Tomographic measurement of local cerebral glucose metabolic rate in humans with (F-18)2-fluoro-2-deoxy-D-glucose: Validation of method. Ann Neurol 1979;6:371–388. [PubMed: 117743]

Rauch SL, Shin LM, Wrigh CI. Neuroimaging studies of amygdala function in anxiety disorders. Ann NY Acad Sci 2003;985:389–410. [PubMed: 12724173]

Rilling JK, Winslow JT, O'Brien D, Gutman DA, Hoffman JM, Kilts CD. Neural correlates of maternal separation in rhesus monkeys. Biol Psychiatry 2001;49(2):146–157. [PubMed: 11164761]

Salomons TV, Johnstone T, Backonja MM, Davidson RJ. Perceived Controllability Modulates the Neural Response to Pain. J Neurosci 2004;24:7199–7203. [PubMed: 15306654]

Schoenbaum G, Setlow B. Lesions of nucleus accumbens disrupt learning about aversive outcomes. J Neurosci 2003;23(30):9833–9841. [PubMed: 14586012]

Sokoloff L, Reivich M, Kennedy C, Des Rosiers MH, Patlak CS, Pettigrew KD, et al. The [14C] deoxyglucose method for the measurement of local cerebral glucose utilization: Theory, procedure, and normal value in the conscious and anesthetized albino rat. J Neurochemistry 1977;28:897–916.

Swanson LW, Cowan WM. The connections of the septal region in the rat. J Comp Neurol 1979;186(4): 621–655. [PubMed: 15116692]

Walker DL, Davis M. Double dissociation between the involvement of the bed nucleus of the stria terminalis and the central nucleus of the amygdala in startle increases produced by conditioned versus unconditioned fear. J Neurosci 1997;17:9375–9383. [PubMed: 9364083]

Walker DL, Toufexis DJ, Davis M. Role of the bed nucleus of the stria terminalis versus the amygdala in fear, stress, and anxiety. Eur J Pharmacol 2003;463:199–216. [PubMed: 12600711]

Woods RP, Grafton ST, Holmes CJ, Cherry SR, Mazziotta JC. Automated image registration I: General methods and intrasubject, intramodality validation. J Comput Assist Tomogr 1998;22(1):139–152. [PubMed: 9448779]

Worsley KJ, Marret S, Neelin P, Evans AC. Searching scale space for activation in PET images. Human Brain Mapping 1996;4:74–90.

Yanagimoto K, Maeda H. The nucleus accumbens unit activities related to the emotional significance of complex environmental stimuli in freely moving cats. Neurosci Res 2003;46(2):183–189. [PubMed: 12767481]

Zald DH, Pardo JV. The neural correlates of aversive auditory stimulation. Neuroimage 2002;16(3 Pt 1): 746–753. [PubMed: 12169258]
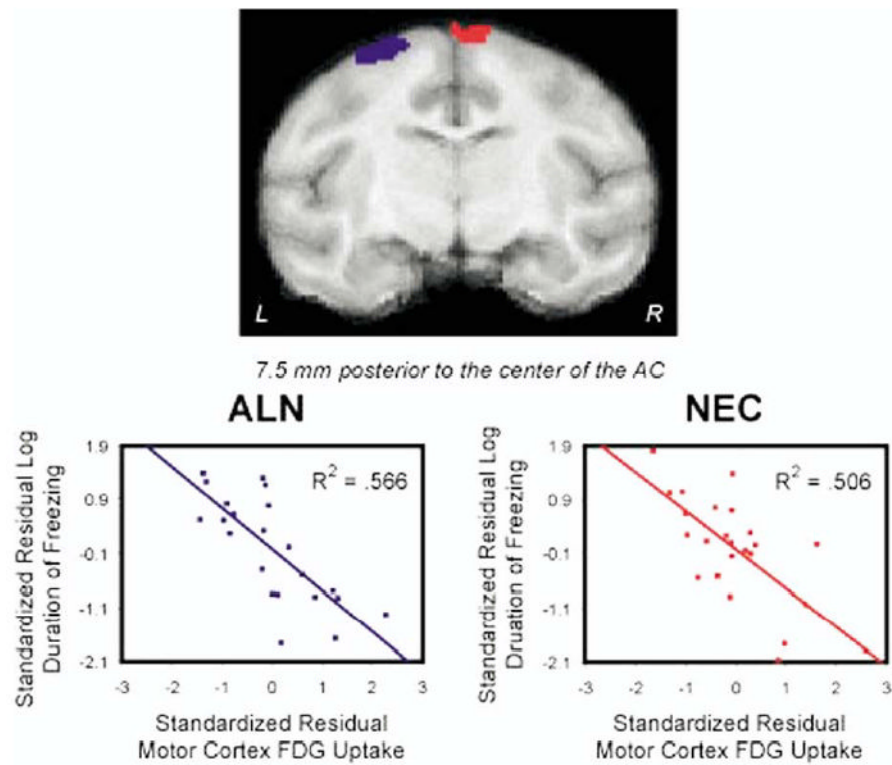
Figure 1.
The duration of freezing behavior (mean log duration of freezing in sec per min + SEM) for the Alone (ALN) compared to the No Eye Contact (NEC) condition. * *p* < .05
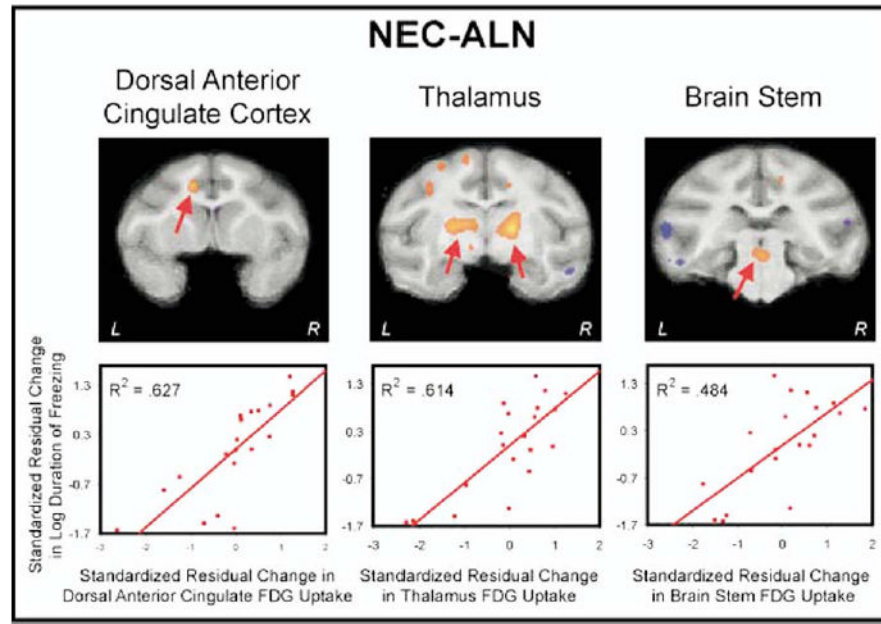
Figure 2.
The BNST/NAC regions that are correlated with freezing duration in the NEC (red) and ALN (blue) conditions are displayed. Regions of interest were defined by voxels that were correlated with the log duration of freezing at an uncorrected threshold of $p < .005$. The correlated regions, overlaid on an MRI template, are depicted in **(A)** an anterior region and in **(B)** a more posterior region of the BNST/NAC area. Corresponding anatomical drawings adapted from a rhesus monkey atlas (Figures 40 and 48) (Paxinos et al 2000) display the location of the nucleus accumbens, bed nucleus of the stria terminalis and the substantia innominata. Scatter plots represent the relation between log freezing duration and brain activity in the BNST/NAC ROIs for the NEC (red) and ALN (blue) conditions. Both variables are standardized and residualized for age. ALN, alone group; NEC, no eye contact group; BNST, bed nucleus of the stria terminalis; NAC, nucleus accumbens; MRI, magnetic resonance imaging; ROI, regions of interest.

Figure 3.
The regions of motor cortex that are correlated with freezing duration in the NEC (red) and ALN (blue) conditions. Regions of interest were defined by voxels that were correlated with the log duration of freezing at an uncorrected threshold of $p <.005$. The correlated regions are overlaid on a slice of an MRI template, which corresponds to Figure 67 of the rhesus monkey atlas (Paxinos et al 2000). Scatter plots represent the relation between log freezing duration and brain activity in the motor cortex ROIs for the NEC (red) and ALN (blue) conditions. Both variables are standardized and residualized for age. ALN, alone group; NEC, no eye contact group; MRI, magnetic resonance imaging; ROI, regions of interest.

Figure 4.
Brain regions (dorsal anterior cingulate cortex, thalamus, and brain stem) in which the change in brain activity is correlated with the change in freezing duration between the NEC and ALN conditions. Regions of interest (ROIs) were defined by voxels that were correlated with the log duration of freezing at an uncorrected threshold of $p < .005$. The correlated regions are overlaid on an MRI template, which correspond to Figures 53, 65, and 83 of the rhesus monkey atlas (Paxinos et al 2000). The ROIs used are highlighted with arrows and scatter plots are presented demonstrating the relation between the change in log freezing duration and the change in brain activity. All the variables are standardized and residualized for age. Other correlated areas are displayed in orange (positive) and blue (negative). ALN, alone condition; NEC, no eye contact condition; MRI, magnetic resonance imaging; ROI, regions of interest.

Table 1

Brain Regions Correlated with Freezing Duration

NEC	Brain Region	mm³	Max *t*	x	y	z
Positive Correlation	BNST/NAC	26.37	6.08	3.125	1.875	−1.25
Negative Correlation	Area 4 (motor ctx), Area 2 (somatosensory ctx), and Parietal areas (PE, POa, PG)	1592.04	6.41	14.375	−18.125	18.125
	White matter bordering ventral Area 46	48.83	4.65	−15	11.875	7.5

AL	Brain Region	mm³	Max *t*	x	y	z
Positive Correlation	BNST/NAC	36.38	4.09	−4.375	2.5	.625
	Lateral Geniculate, External Medullary Lamina, Reticular Thalamic Nucleus	26.37	4.32	15	−14.375	−1.25
	White Matter bordering PG associated area of the superior temporal sulcus	9.52	3.38	−17.5	−3.125	−6.875
Negative Correlation	Areas 1, 2, 3 (somatosensory ctx), Area 4 (motor ctx)	156.25	5.00	−11.25	−10	22.5
	Area 2 (somatosensory ctx)	45.41	4.33	−1.875	−16.25	17.5
	Area 4 (motor ctx)	27.34	3.91	−16.25	−5	16.25
	Parietal Area PEa	15.63	4.11	−15	−15	16.875
	Area 4 (motor ctx)	13.92	3.48	17.5	−5	15.625
	Parietal Area PEa	11.96	3.70	15	−14.375	15.625

Significant (*p* <.005 uncorrected) clusters resulting from a voxelwise correlation between brain activity and log duration of freezing behavior controlling for age in the NEC and ALN conditions. All clusters larger than 8 mm³ are included. (Posterior regions of the brain were excluded as described in the Methods and Materials.) Anatomical definitions of the clusters were made based on the rhesus monkey atlas (Paxinos et al 2000). Data presented include the size of the cluster (mm³), the maximum *t*-value within the cluster, and the corresponding x (left to right), y (posterior to anterior) and z (inferior to superior) coordinates in mm relative to the center of the anterior commissure. The clusters are presented in descending order based on their size. ALN, alone group; NEC, no eye contact group; BNST, bed nucleus of the stria terminalis; NAC, nucleus accumbens; MRI, magnetic resonance imaging; ROI, regions of interest.

Table 2

Brain Regions Correlated with the Regulation of Freezing

NEC-ALN	Brain Region	mm^3	Max t	x	y	z
Positive Correlation	Lateral ventral thalamic nucleus and reticular Thalamic Nucleus (Left)	116.70	4.62	−8.75	−5.625	3.75
	Lateral ventral thalamic nucleus and reticular Thalamic Nucleus (Right)	95.46	6.08	6.875	−5.625	3.125
	Areas 24c and Area 6/32	24.41	5.54	−5.625	3.75	14.375
	Brain stem (dorsal raphe nucleus)	20.51	4.25	−.625	−14.375	−4.375
Negative Correlation	Genu of corpus collosum	45.41	5.53	.625	10	8.125
	Temporal parieto-occipital associated area in the Superior Temporal sulcus, middle temporal area (V5), fundus of superior temporal sulcus	36.13	3.80	21.875	−19.375	6.25
	Area 8, Anterior Ventral Part	28.08	4.17	17.5	5	11.875
	Parietal area PE; PG associated area of the superior temporal sulcus	13.92	3.97	18.125	−13.75	15.625
	Granular insular cortex	11.96	3.95	18.75	−5.625	4.375
	Temporal parieto-occipital associated area in the Superior Temporal sulcus	10.25	3.70	−26.25	−15	2.5

Significant ($p < .005$ uncorrected) clusters resulting from a voxelwise correlation between the change in brain activity and change in log duration of freezing behavior controlling for age between the NEC and ALN conditions. All clusters larger than 8 mm^3 are included. (Posterior regions of the brain were excluded as described in the Methods and Materials.) Anatomical definitions of the clusters were made based on the rhesus monkey atlas (Paxinos et al 2000). Data presented include the size of the cluster (mm^3), the maximum t-value within the cluster, and the corresponding x (left to right), y (posterior to anterior) and z (inferior to superior) coordinates in mm relative to the center of the anterior commissure. The clusters are presented in descending order based on their size. ALN, alone group; NEC, no eye contact group.